

## USING MATHEMATICAL MORPHOLOGY TO ELIMINATE DEBRIS AND AGGREGATES BEFORE DNA PLOIDY MEASUREMENT OF SOLID TUMOURS

Christophe Boudry<sup>1,2,3</sup>, Paulette Herlin<sup>2</sup>, Michel Coster<sup>1</sup>, Jean-Louis Chermant<sup>1</sup>,  
Brigitte Sola<sup>3</sup>, Michel Henry-Amar<sup>4</sup>

<sup>1</sup>LERMAT, URA CNRS 1317, ISMRA, 14050 Caen Cedex, France

<sup>2</sup>Centre F. Baclesse, Service d'Anatomie Pathologique, 14021 Caen, France

<sup>3</sup>Université de Caen, URA CNRS 1829, 14074 Caen, France

<sup>4</sup>Centre F. Baclesse, Service de Recherche Clinique, 14021 Caen, France

### ABSTRACT

Software strictly dedicated to DNA tumour measurement was previously developed, providing an automatic sorting of cellular elements based on a multiparametric analysis. Prospective research now focuses on the simplification of the sorting procedure. Mathematical morphology was used for pre-elimination of debris and aggregates. The results were compared to those obtained with multiparametric analysis. It is concluded that mathematical morphology is a promising tool.

**Key words:** aggregates, debris, DNA ploidy measurement, mathematical morphology, solid tumours.

### INTRODUCTION

Flow cytometry has been widely used to evaluate DNA content of archival tumours. Though this technique allows the measurement of large populations of nuclei in a short amount of time, it is a well-known "blind" technique which is unable to eliminate, in a simple and reliable way, unwanted cell categories such as inflammatory and stromal elements as well as debris generated by dewaxing. Image analysis, an alternative tool for DNA quantification, allows sorting of unwanted elements under visual control, but is reputed to be time consuming and unable to give statistically valuable results in an acceptable delay in clinical oncology (Lee et al., 1994). Since the last "consensus review of the clinical utility of DNA cytometry of the breast" recommended the elaboration of fully automatic image cytometers (Hedley et al., 1993), software strictly dedicated to this task was developed in Caen. It offers automatic sorting of cellular elements based on a multiparametric analysis (MA) by reference to a specific knowledge base (Masson et al., 1994). Technical research now focuses on the simplification of the sorting procedure in order to save further time and compete with flow cytometry. For this task, specific programs for pre-elimination of debris and aggregates based on mathematical

morphology (MM) were developed. Preliminary results are presented and compared with those obtained with MA.

## MATERIAL AND METHODS

### Biological material

The study was done on archival brain tumours corresponding to one case of astrocytoma grade 2 (Ast2), one case of astrocytoma grade 3 (Ast3), one case of glioblastoma multiform (Gbm) and one case of medulloblastoma (Med). 50  $\mu\text{m}$  thick paraffin sections were prepared according to Van-Driel Kulker et al. (1987) and DNA stained according to Feulgen and Rossenbeck (1924) as described previously (Herlin et al., 1992).

### Image cytometry

The image cytometer consists of a BH2 Olympus microscope, a moving stage, a matrox PIP 1024 frame grabber and a Sony CCD camera. Integrated optical density measurements were done at a resolution of  $512 \times 512$  pixels in 8 bits (1 pixel =  $0.11 \mu\text{m}^2$ ) from the rectangular frame of the recorded image. The same sequences of stored images (200 images of normal tissue and 50 images of each tumour) were used to compare sorting procedures. The software for DNA measurement and sorting by MA, implemented on PC and workstations, has been written in C language and runs under the UNIX operating system. Visilog 4 software (Noesis France) also running under the UNIX operating system provided mathematical morphology routines.

### Sorting methods

- *Manual sorting* (reference): For each tumour, sorting of the various nuclear elements was done manually assuming they corresponded to the reference. Segmented events were classified in eleven categories of normal nuclei, abnormal nuclei and debris. This manual sorting allowed an estimation of the percentage of each nuclear category, debris and aggregates for each tumour. About 1000 elements per tumour were studied.

- *Automatic sorting by MA*: This method is based on the multiparametric analysis of 38 parameters calculated on each segmented element (size, texture and intensity) and on learning of nuclear morphology. A knowledge base was obtained by manual sorting of well preserved nuclei. Debris and aggregates represented the sorting group by deficit (not learned). Automatic sorting for each tumour was done by reference to its own knowledge base.

- *Automatic sorting by MM*: For this preliminary approach, the automatic method developed allows the classification of all the undamaged nuclei in one group, as opposed to another group of debris and aggregates. After transformation of the rectangular frame of the recorded image to an hexagonal one (Serra and Lay, 1984), an area filter is used to characterize debris smaller than the smallest nuclei. Four form parameters were tested to characterize aggregates and larger debris:

- **p2a**: the classical parameter obtained from the calculation of the area ( $A_i$ ) and perimeter ( $P_i$ ) of the initial particle:

$$p2a = (P_i)^2 / (4 \times \pi \times A_i).$$

- **gl**: the index of geodesic lengthening (Lantuejoul and Maisonneuve, 1984):

$$gl = (4 \times A_i) / \pi \times (\text{geodesic diameter})^2.$$

- **Pci**: perimeter concavity index which corresponds to the sum of the Feret diameters ( $F$ ) divided by the sum of intercepts ( $I$ ) in the three directions of the hexagonal frame. Calculation of intercepts on the hexagonal convex hull is used to determine  $F$  (Figure 1).

- **Aci**: area concavity index which corresponds to the initial area ( $A_i$ ) divided by the area of the hexagonal convex hull ( $A_c$ ) of segmented elements (Figure 1). Since the correlation coefficient between the real convex hull (Sati and Laroye, 1994) and the hexagonal one calculated using linear regression for Ast2 was 0.82 ( $p < 0.001$ ,  $n = 1079$ ), the hexagonal convex hull was used allowing time saving.

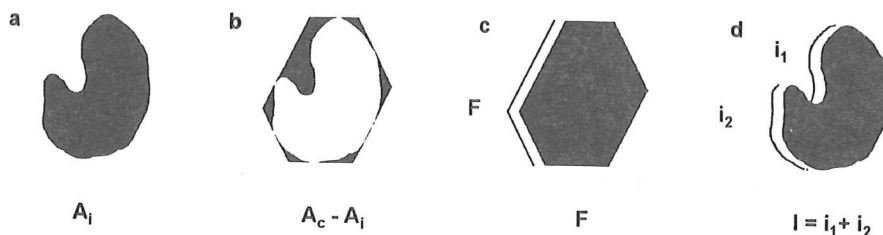


Fig. 1. Calculation of  $A_{ci}$  and  $P_{ci}$ : (a) Initial area; (b) difference between the area of hexagonal convex hull and initial area; (c) representation of the Feret diameter of the particle (corresponding to the intercepts of convex hull); (d) intercepts of the particle in the horizontal direction.

To determine a sorting model for each tumour, the distribution of each parameter was first divided in quintiles. The proportions of debris and aggregates versus undamaged nuclei were compared between quintiles with the chi-square test. Threshold values retained for each parameter were those which gave the best contrast. Using a logistic regression model (Pagano and Gauvreau, 1993), the combination of thresholds of the more pertinent parameters ( $p < 0.05$ ) permitted to characterize a population of undamaged nuclei against a population of debris and aggregates. The combination which gave a proportion of debris and aggregates greater than or equal to 50 % was used for sorting models.

#### Evaluation of performances of the 2 automatic methods by reference with manual sorting

- *Global comparison*: The sensitivities ( $Q_i$ ) representing the global sorting quality of the methods used were first compared. The sensitivity is defined as the percentage of debris and aggregates correctly classified by automatic methods by reference to manual sorting:

$$Q_i = 100 \times (N_{\text{manu}} \cap N_{\text{auto}}) / N_{\text{manu}}$$

where  $N_{\text{manu}}$  and  $N_{\text{auto}}$  are the numbers of debris and aggregates obtained by manual and automatic sorting, respectively.

The false positive (FP) rate is defined as the percentage of undamaged nuclei misclassified as debris and aggregates. 95 % confidence intervals for  $Q_i$  and FP rates were calculated assuming a binomial distribution of rates.

- *Cell by cell comparison*: For each nuclear category, the number and proportion of false positives were calculated. The exact Fischer test was used to assess if the proportion of debris and aggregates in each nuclear category was independent of nuclear category itself.

- *DNA histogram comparison*: DNA ploidy histograms were built after elimination of debris and aggregates by manual and automatic methods. DNA ploidy distribution of false positive events was also evaluated.

#### Evaluation of the concordance between the 2 automatic methods, cell by cell comparison

The concordance factor  $Q_c$  was calculated as follows:

$$Q_c = 100 \times (n \text{ MA} \cap n \text{ MM}) / 0.5 \times (n \text{ MA} + n \text{ MM})$$

where  $n \text{ MA}$  and  $n \text{ MM}$  are the numbers of debris and aggregates obtained by MA and MM sorting, respectively.  $Q_c$  represents the cell by cell comparison of labeling by the 2 automatic methods used.

## RESULTS

After the manual sorting, debris and aggregates represented 46 to 75 % of the segmented elements from the tumours studied.

#### Automatic elimination of debris by MM compared with manual elimination

As the analysis has shown that  $gl$  was useless to characterize debris and aggregates, this parameter was no longer used in the models.

Sensitivities and the FP rates obtained with MM are given in Table 1 (a).

Table 1. MM (a) and MA (b) sorting. 95% confidence intervals are given in parentheses.

a	#	MM		b	#	MA	
		Sensitivity ( $Q_i$ )	False positive			Sensitivity ( $Q_i$ )	False positive
Ast2	1079	78% (75-82)	22% (19-27)	Ast2	1079	77% (73-80)	20% (16-24)
Ast3	766	90% (87-93)	24% (20-30)	Ast3	766	90% (87-93)	23% (19-29)
Gbm	1441	83% (80-85)	41% (36-46)	Gbm	1441	81% (78-83)	27% (23-37)
Med	887	66% (61-70)	26% (22-31)	Med	887	62% (57-66)	10% (7-13)

# represents the number of elements analyzed.

Whatever the tumour, FP events were not generated in the same proportions in the eleven nuclear categories ( $p < 0.005$ ) (data not shown). FP events were more numerous in abnormal nuclear categories (mean = 39 %) than in normal ones (mean = 22 %).

Figure 2 presents DNA curves obtained for Ast2 case. On one hand, the proportion of nuclei in the tetraploid range was lower after MM sorting (17.2 %) (Figure 2c) than after manual sorting (22 %) (Figure 2b). On the other hand, the proportion of nuclei in the diploid range was higher after MM sorting (81.6 %) than after manual sorting (76.6 %). Ploidy curve

of FP events showed that the proportion of nuclei in the tetraploid range is important after MM (33.9 %) (Figure 2d).

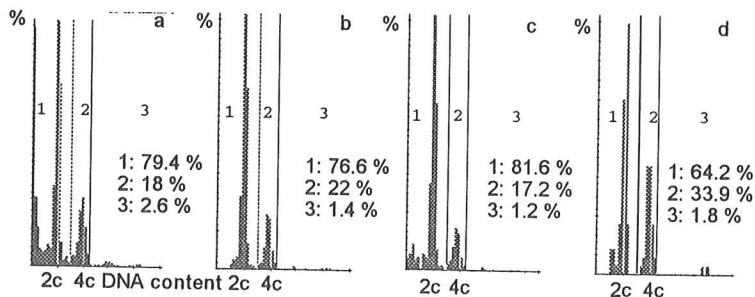


Fig. 2. *Astrocytoma grade 2.* (a) Crude DNA histogram (undamaged nuclei, debris and aggregates); (b) DNA histogram of undamaged nuclei after manual elimination of debris and aggregates; (c) DNA histogram of undamaged nuclei after elimination of debris and aggregates by MM; (d) DNA histogram of false positive generated by MM.

### Automatic elimination of debris by MA compared with manual elimination

Global results obtained with MA are presented in Table 1b.

These results did not statistically differ from those obtained with MM (Table 1a). Extraction of FP events in the eleven nuclear categories was not randomly observed ( $p < 0.005$ ) for the four studied tumours (data not shown). FP events were more numerous in normal nuclear categories (mean = 27 %) than in abnormal ones (mean = 23 %).

The elimination of debris and aggregates for Ast2 is given in Figure 3. Results must be compared with that of manual sorting (Figure 2b).

Nuclei situated in the tetraploid range represented 29.4 % after elimination of debris and aggregates by MA (Figure 3a) as compared with 22 % after manual sorting (Figure 2b).

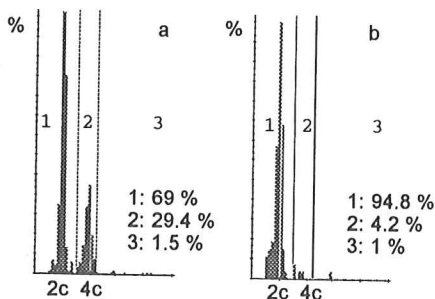


Fig. 3. *Astrocytoma grade 2.* (a) DNA histogram of undamaged nuclei after elimination of debris and aggregates by MA; (b) DNA histogram of false positives generated by MA.

Moreover, the proportion of nuclei situated in the diploid range was lower after MA than after manual sorting.

Ploidy curve of FP events showed that the proportion of nuclei in the tetraploid range is very low after MA (4.2 %) (Figure 3b).

#### Agreement between the 2 automatic methods

The percentage of elements labelled as debris and aggregates by the 2 automatic methods (agreement rates Qc: 73 % for Ast2, 87 % for Ast3, 80 % for Gbm and 68 % for Med) was relatively low considering the similarity of their sensitivities.

## DISCUSSION AND CONCLUSION

Software dedicated to automatic DNA measurements previously developed in our laboratory allows a fully automatic sorting of cellular elements based on multiparametric analysis (MA). This method gives fairly good results, but needs to be improved for nuclear debris and aggregates (Masson et al., 1994). To further introduce image analysis DNA measurements into routine clinical oncology, research now focuses on simplification of the sorting procedure in order to save time while increasing efficiency.

The principle of mathematical morphology (MM) is to compare analyzed structures to elements with well known geometry. To the best of our knowledge, most classification tools used in biology are based on the calculation of parameters excluding image transformations (Wheless and Robinson, 1994, Pauwels and Kiss, 1994); in addition, parameters derived directly from MM such as **gl**, **Pci** and **Aci** are rarely used. In examples of MM utilization reported in the literature, global transformations are applied on images without calculating parameters (Meyer, 1979, Gimenez-Mas et al., 1995). In the present study, parameters derived from MM were used because they allow statistical analysis and offer the possibility to practice sorting in reference to a knowledge base.

The parameter **gl**, which describes the lengthening and the global shape of elements and is a robust parameter, could have been useful to characterize debris and aggregates, but the statistical analysis has shown a lack of adequacy to our data. The parameter **p2a** which is not very robust (Coster and Chermant, 1989) and is too general to be very selective, was used because of its simplicity and disclosed efficiency for the models. The statistical analysis also showed that **Pci** and **Aci**, which allow a robust estimation of concavity of particles were useful.

Results of new methods have to be evaluated and compared with the existing ones before their introduction in the software. For this evaluation, manual sorting is the only standard available despite its lack of reproducibility. Comparison must concern the quality of global results (i.e. cell by cell labelling) as well as the persistence of the pertinent information (i.e. ploidy curves). As a matter of fact, the comparison between MM and MA showed that even these methods have the same global performances, the pertinent information (ploidy abnormality) is not restored in the same way.

The results presented in this paper show that the method developed using MM is promising for pre-elimination of debris and aggregates (simplicity, global performances) even if the approach requires further improvements. In particular, the use of grey level images could reduce the disadvantages of the method proposed using functional MM in addition to binary MM.

## ACKNOWLEDGMENTS

The authors wish to thank J.P. Signolle, B. Plancoulaine and F. Duigou for their participation in this work. This work was done under the auspices of "Pôle Traitement et Analyse d'Images de Basse Normandie". Christophe Boudry is a fellowship of "Ministère de l'Enseignement Supérieur et de la Recherche".

## REFERENCES

- Coster M, Chermant JL. *Precis d'analyse d'images*. (1989), Les Presses du CNRS.
- Feulgen R, Rossenbeck H. Mikroskopisch chemischer Nachweis einer nucleinsäure von typus der thymonucleinsäure und die darauf beruhende elektive färbung von zellkernen in mikroskopischen präparaten. *Z Physiol Chem* 1924; 135: 203-24.
- Giménez-Mas J, Sanz-Moncasi M, Remon L, Gambo P, Gallego-Calvo MP. Automated textural analysis of nuclear chromatin. A mathematical morphology approach. *Analyt Quant Cytol Histol* 1995; 17: 39-47.
- Hedley DW, Clark GM, Cornelisse CJ, Killander D, Kute T, Merkel D. Consensus review of the clinical utility of DNA cytometry in carcinoma of the breast. *Cytometry* 1993; 14: 482-5.
- Herlin P, Duigou F, Masson E, Bloyet D, Mandard AM. Image analysis optimization for the routine retrospective measurement of DNA ploidy of solid tumors Part II : Applications and output. *Acta Stereol* 1992; 11: 411-7.
- Lantuejoul C, Maisonneuve F. Geodesic methods in quantitative image analysis. *Patt Recogn* 1984; 17: 177-87.
- Lee S, Tolmachoff T, Marchevsky M. DNA content analysis ("Ploidy") by image analysis. In: Marchevsky M, Bartels PH, eds. *Image Analysis: A Primer for Pathologists*. New York: Raven Press, 1994: 261-307.
- Masson E, Herlin P, Galle I, Duigou F, Belhomme P, Bloyet D, Mandard AM. Automatic classification of cellular elements of solids tumors: application to DNA quantitation. *Acta Stereol* 1994; 13: 75-81.
- Meyer F. Iterative image transformation for automatic screening of cervical smears. *J Histochem Cytochem* 1979; 27: 128-35.
- Pagano M, Gauvreau K. *Principles of Biostatistics*. Belmont CA: Duxbury Press, 1993.
- Pauwels O, Kiss R.. Computerized morphonuclear analyses of Feulgen-stained nuclei from 11 chemosensitive and from 11 chemoresistant neoplastic cell lines. *Analyt Cell Pathol* 1994; 7: 235-50.
- Sati M, Laroye GJ. A simple algorithm for measuring the concavity/convexity ratio and lobe counting of a close curve. *Analyt Quant Cytol Histol* 1994; 16: 269-83.
- Serra J, Lay B. Square to hexagonal lattices conversion. *Rapport du Centre de Géostatistique et de Morphologie Mathématique, Ecole des mines, Fontainebleau, n° 888, 1984.*

- Van Driel-Kulker AMJ, Mesker WE, Van der Burg MJM, Ploem JS. Preparation of cells from paraffin-embedded tissue for cytometry and cytomorphologic evaluation. *Analyt Cell Pathol* 1987; 9: 225-31.
- Wheless L, Robinson R. Classification of red blood cells as normal, sickle, or other abnormal, using a single image analysis feature. *Cytometry* 1994; 17: 159-66.